

## SYNTHESIS AND CHARACTERIZATION OF CHITOSAN/PHOSPHOTUNGSTIC ACID - MONTMORILLONITE MODIFIED BY SILANE FOR DMFC MEMBRANE

Dian Permana<sup>1</sup>, Muhammad Purwanto<sup>1</sup>, La Ode Ahmad Nur Ramadhan<sup>2</sup>, and Lukman Atmaja<sup>1,\*</sup>

<sup>1</sup>Department of Chemistry, Sepuluh Nopember Institute of Technology (ITS)  
Jl. Arief Rahman Hakim, Sukolilo, Surabaya 60111 Indonesia

<sup>2</sup>Department of Chemistry, Halu Oleo University  
Jl. Kampus Hijau Bumi Tridharma, Anduonou, Kendari 93132, Southeast Sulawesi Indonesia

Received 9 October, 2014; Accepted May 7, 2015

### ABSTRACT

Montmorillonite was functionalized by (3-glycidyloxypropyl) trimethoxy silane (GPTMS). Subsequently, chitosan (CS) membranes filled by GPTMS-modified montmorillonite particles were prepared and characterized by FTIR. The result of FTIR obtained the peak wavenumber of 2940, 1471 and 1390  $\text{cm}^{-1}$  referring to vibration stretching of  $\text{CH}_2$ , bending of  $\text{CH}_2$  and  $\text{CH}_3$  form epoxy groups in silane, respectively which indicated modification of montmorillonite by silane. Compared with the pure CS and CS/PWA-MMT membrane, these CS/PWA-MMT/Silane hybrid membranes show apparently high proton conductivity and the lower methanol permeability, which could be assigned to the better interfacial morphology and compatibility between chitosan matrix and GPTMS-modified montmorillonite. In all the prepared CS/PWA-MMT/Silane hybrid membranes, the CS membrane filled by 10% GPTMS-modified montmorillonite particles exhibits the highest proton conductivity and the lowest methanol permeability, which is  $19.15 \times 10^{-3} \text{ S.cm}^{-1}$  at 80 °C and  $4.33 \times 10^{-8} \text{ cm}^2.\text{s}^{-1}$ , respectively. The results imply that CS/PWA-MMT silane 10% membrane has better interaction of interfacial morphology and compatibility between chitosan matrix and GPTMS-modified montmorillonite particles.

**Keywords:** chitosan; membrane; montmorillonite; proton conductivity; methanol permeability

### ABSTRAK

Montmorillonit dimodifikasi dengan (3-glycidyloxypropyl) trimethoxy silane (GPTMS). Selanjutnya, membran kitosan terisi oleh partikel monmorilonit termodifikasi GPTMS dibuat dan dikarakterisasi menggunakan FTIR. Hasil FTIR diperoleh puncak pada bilangan gelombang 2940, 1471 dan 1390  $\text{cm}^{-1}$  merupakan vibrasi stretching  $\text{CH}_2$ , bending  $\text{CH}_2$  dan  $\text{CH}_3$  gugus epoksi pada silan yang mengindikasikan modifikasi monmorilonit oleh silan. Dibandingkan dengan membran CS murni dan CS/PWA-MMT, membran hybrid CS/PWA-MMT/Silan ini memperlihatkan konduktivitas proton yang tinggi dan permeabilitas metanol yang rendah, yang menandakan bahwa interaksi morfologi dan kompatibilitas yang sangat baik antara matriks kitosan dan monmorilonit termodifikasi GPTMS. Pada semua membran hybrid CS/PWA-MMT/Silan, membran CS yang diisi dengan partikel monmorilonit/silan 10% memperlihatkan konduktivitas proton tertinggi dan permeabilitas metanol terendah yakni berturut-turut  $19,15 \times 10^{-3} \text{ S.cm}^{-1}$  pada suhu 80 °C dan  $4,33 \times 10^{-8} \text{ cm}^2.\text{s}^{-1}$ . Hasil menyatakan bahwa membran CS/PWA-MMT 10% memiliki interaksi yang paling baik morfologi antarmuka dan kompatibilitas antara matriks kitosan dan partikel monmorilonit termodifikasi silan.

**Kata Kunci:** kitosan; membran; monmorilonit; konduktivitas proton; permeabilitas metanol

### INTRODUCTION

The development about new sustainable and economical energy source with low emission has been attracting much attention recently to overcome environmental pollution and global warming. In this regard, fuel cell technology as a promising candidate has attracted considerable interest during the past years. Fuel cells, as eco-friendly electrical energy generation

system, are able to direct convert chemical energy to electricity via redox reaction with reduced adverse environmental impact [1].

Polyelectrolyte membranes (PEMs), as the key part of such systems, have crucial role as the transport medium for generated protons from oxidation of fuel [2-3]. Organic-inorganic hybrid membrane has attracted much attention as proton exchange membrane (PEM) for direct methanol fuel cell (DMFC) recently. The

\* Corresponding author. Tel/Fax : +62-81233116041  
Email address : lukman.at@gmail.com

presence of inorganic moiety can significantly enhance methanol rejection, the thermal and mechanical stability of the hybrid membrane [4]. There are many kinds of inorganic fillers, such as silica, titanium oxide, zirconium oxide, aluminum oxide, montmorillonite, heteropoly acid and zeolite [5-12] have been employed to develop organic-inorganic hybrid membranes for DMFC application.

Nafion is currently the most commonly utilized proton exchange membrane (PEM) for DMFCs because of superior chemical stability and high proton conductivity. However, it still has some drawbacks such as reduction in conductivity at high temperature, high methanol permeability and high production cost [13]. Therefore, the development of new alternative hybrid membranes that will provide improved character, environmental benign, and low production cost for fuel cell application is highly required. The new DMFCs membranes require several important properties, including good film formation, high methanol rejection, good mechanical stability and hydrophilic character to allow sufficient ionic conductivity [14-15].

Chitosan (CS), a polysaccharide bio resource, has been attracting considerable interest to substitute Nafion as DMFCs in fuel cell application [16]. It was pointed out that cationic polyelectrolyte such as chitosan has unique character due to the presence of both amine and hydroxyl groups [17]. Although it has low ionic conductivity compared to Nafion, but it has low methanol permeability. Therefore, it makes chitosan membrane an excellent material to be further developed [18].

In this study, DMFCs membranes were prepared from mixture of chitosan (CS) as matrix and modified-montmorillonite (MMT) with different concentration of silane. Meanwhile, phosphotungstic acid as complex agen for enhances proton conductivity of hybrid membrane. Hopefully, the formation of polyelectrolyte hybrid composite membrane from both CS/PWA and modified-montmorillonite is expected to improve its conductivity, rejecting methanol and thermal stability. The aim of this research is to study the applicability of this polyelectrolyte complex-composite membrane, for DMFC by analysis the proton conductivity, methanol permeability, water and methanol uptake, and to elucidate interaction between matrix and filler.

## EXPERIMENTAL SECTION

### Materials

Chitosan with a deacetylation degree of 81% was supplied by CV. Bio Chitosan Indonesia. Montmorillonite K-10 (surface area: 220-270 m<sup>2</sup>/g), (3-glycidylpropyl)trimethoxy silane (GPTMS) and phosphotungstic acid hydrate (P4006-25G) were purchased from Sigma-

Aldrich. Acetic acid, methanol, hydrochloride acid, and *N, N*-dimethyl formamide (DMF) were purchased from Merck. Sodium hydroxide was purchased locally. De-ionized water was used in all experiments.

### Instrumentation

Fourier transform infrared spectroscopy (4,000-500 cm<sup>-1</sup>, resolution 4 cm<sup>-1</sup>) and *Impedance Analyzer* (Agilent™ E4980A).

### Procedure

#### *Modification of montmorillonite*

Montmorillonite was modified by silane according to the procedure describe in the literature [19]. Montmorillonite and 3-glycidylpropyltrimethoxy silane (5, 10 and 15%) were dissolved in dimethyl formamide and then stirred at room temperature for 6 h. Subsequently, the homogenous solution put into oven at 60 °C for 24 h. The reaction be continued at 100 °C for 1 h and then at 120 °C for 2 h. After that, 1 M hydrochloride acid was added to the dry products at 80 °C for 24 h. The products were denoted as MMT-silane 5%, MMT-silane 10% and MMT-silane 15%.

#### *Membrane preparation*

75 g 2.0 wt% aqueous solution of acetic acid was equally divided into two portions. 1.5 g CS powders were dissolved in one portion of acetic acid solution at 80 °C. A certain amount of montmorillonite was dispersed in the portion of acetic acid solution by ultrasonic treatment for 30 min. Subsequently, two portions of solution were mixed, and stirred at 80 °C for 30 min. Then, ultrasonic treatment and stirring were carried out alternatively, each for 30 min. After thorough degasification, the mixture was cast onto clean glass plate and dried at room temperature for 72 h. Next, 1 N sodium hydroxide solution was added to the dry membranes in the Petri dishes several times. The neutralized membranes were washed several times with deionized water and soaked in PWA solution 2% for 24 h. Then, the membranes were washed and immersed in deionized water for 24 h to remove the physically absorbed PWA. Finally, the membranes were dried at 25 °C. The thickness of all membranes was in the range of 1.5 to 1.7 (10<sup>-4</sup>) cm. The membranes were denoted as CS/PWA, CS/PWA-MMT, CS/PWA-MMT/Sil 5%, CS/PWA-MMT/Sil 10% and CS/PWA-MMT/Sil 15%.

#### *Water and methanol uptake measurements*

The water and methanol uptake of membrane were determined by measuring the weight difference of membrane before and after immersion in water or an

aqueous solution of methanol. Membrane samples dried at room temperature for 24 h were weighted, and the immersed in water or 5 mol L<sup>-1</sup> aqueous solution of methanol at room temperature for 24 h. After remove residual water or methanol solution on the surface membrane, the wet membrane was weighted. The water and methanol uptake calculated based on Eq. 1:

$$\text{Water uptake, \%} = \frac{M_{\text{wet}} - M_{\text{dry}}}{M_{\text{dry}}} \times 100 \quad (1)$$

Where,  $M_{\text{wet}}$  and  $M_{\text{dry}}$  are the weights of the membrane in the wet and dry states, respectively.

### Proton conductivity

Proton conductivity of fully hydrate membranes were measured as a function of temperature. Measurements were carried out in two point-probe conductivity cells using two platinum wire electrodes as working electrode. The electric resistance data were obtained using impedance analyzer (Agilent™ E4980A) and were recorded between 20 Hz–2 MHz at working voltage amplitude of 1 V. The impedance spectra were fitted on ZView 2 software by Scribner Associates Inc. for curve fitting procedure. The proton conductivity values were obtained according to Eq. 2:

$$\sigma = \frac{S}{R \times A \times L} \quad (2)$$

Where  $S$  is gap of electrodes,  $A$  is wide of electrodes,  $L$  is thickness of membrane and  $R$  is membrane resistance derived from the low intersection of the high frequency semicircle on a complex impedance plane with  $\text{Re}(z)$  axis.

### Methanol permeability

Methanol permeability was measured by means of a two compartment glass diffusion cell. The first cell contained pure methanol (cell A) and the second one contained deionized water (cell B); a mixer stirred both solution continuously to make them homogeneous. The concentration of alcohol diffused from cell A and B across the membranes were examined with time using density meter. The amount of 10 mL was sampled from the cell B every 20 min. Before the permeation experiment, the calibration curve of the density vs. the methanol concentration was prepared. The calibration curve was used to calculate the methanol concentration in the permeation experiment. The methanol permeability was calculated from the slope of the straight-line plot of alcohol concentration vs. the permeation time. The methanol concentration in the cell B as a function of time is given in Eq. 3 [20]:

$$C_B(t) = \frac{A \times DK}{V \times L} C_a(t - t_0) \quad (3)$$

Where  $C$  is the alcohol concentration,  $A$  and  $L$  are the polymer membrane area and thickness;  $D$  and  $K$  are the

alcohol diffusivity and partition coefficient between the membrane and the solution. The product  $DK$  is the membrane permeability ( $P$ ),  $t_0$  also termed time lag, which is related to the diffusivity;  $t_0 = L^2/6D$ .

## RESULT AND DISCUSSION

### Modification of Montmorillonite

Generally, two main methods were used in the modification of clay surface, i.e., physical and chemical methods [21]. The most method used for modifying clay minerals is using silanes as silicon source in the synthesis of clay minerals [22]. Silane grafting, also known as silylation, was proven to be an efficient method to modify clay minerals surface. Silanes are anchored onto clay mineral surfaces through condensation reaction between the hydroxyls in hydrolyzed silanes and the silanol groups on clay mineral surfaces.

According to literature [22] silylation consist of four steps; the first step is hydrolysis reaction between silane and water molecules in montmorillonite or atmosphere. The existence of water molecules induced formation of silanol groups (Si-OH) which contribute as reactive side to the next step. The second step, silanol groups change to polysilane band within oxane band (Si-O-Si) and lost the water molecules. The next step is grafting of silane in montmorillonite at 100 and 120 °C. In this step, hydrogen bonding occur between hydroxyl groups from polysilane and silanol groups from montmorillonite. The last step is activation of montmorillonite surface using hydrochloride acid at 80 °C.

In this study, montmorillonite was modified by 3-glycidyloxypropyl)trimethoxy silane (GPTMS). The aryloxy groups (O-CH<sub>3</sub>) at one end of the silane can be hydrolyzed into silanol groups (Si-OH) and then co-condensed with the hydroxyl groups (-OH) on the montmorillonite surface.

The FTIR spectra of Na-Mt and the silane grafted montmorillonites are shown in Fig. 1. The spectra shows the peak at 3455 and 1084 cm<sup>-1</sup> corresponding to stretching vibration of the surface hydroxyl groups and stretching vibration of Si-O-Si in montmorillonite, respectively. After silane grafting reaction, intensity of -OH band decrease. It is indicated silane molecules participated in the grafting reaction. New peaks at 2940, 1471 and 1390 cm<sup>-1</sup> referring to vibration stretching of CH<sub>2</sub>, vibration bending of CH<sub>2</sub> and CH<sub>3</sub> form epoxy groups in silane, respectively. These peaks indicated the presence of GPTMS in modified clays. In addition, the peak absorption at 3455 cm<sup>-1</sup> decreased due to consumption of hydroxyl groups to form silanol groups (Si-OH). This result deduces that montmorillonite

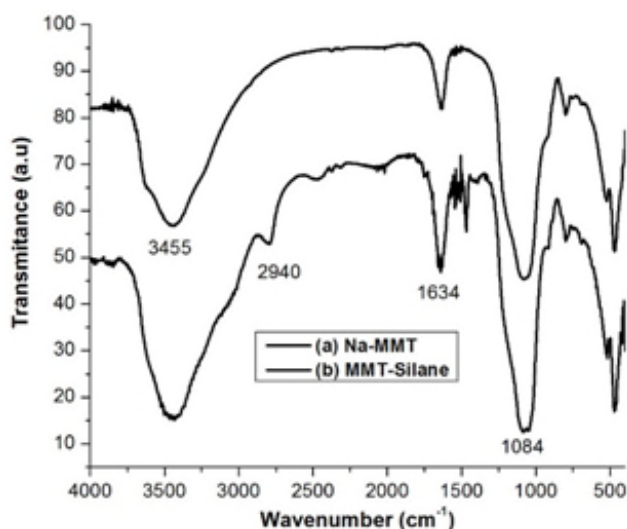


**Fig 1.** FT-IR spectra of montmorillonite before and after modified by silane

was success modified by silane (GPTMS).

### Membrane Formation of CS/PWA-MMT Modified Silane

The synthesis of hybrid composite membranes was carried out by phase inversion method. The substances were dissolved in acetate acid 2% aqueous solution (the same volume). According to the literature [23], the mass composition ratio between chitosan matrix and modified-montmorillonite is 98% : 2% (total weight of 1.5 g). It is the best composition with the best performance in DMFC application.

Basically, the compatibility between matrix polymer and the surface of the inorganic filler is the key issue in determining the final membrane property and performance. The transitional phase is expected to be created between the organic and inorganic phases to improve the interfacial morphology in hybrid membrane, and also migrating or eliminating the nonselective voids. After modification, the organosilane “arms” ( $-\text{CH}_2-\text{CH}_2-\text{CH}_2-\text{Si}\equiv$ ) were grafted on to montmorillonite surface with hydroxyl groups liked to at the end of these “arms” like “hands”. When these modified montmorillonite were blended with the rigid glassy chitosan, the  $-\text{OH}$  were expected to grasp the polymer chains around via hydrogen bonds with the  $-\text{NH}_2$  groups on chitosan. Moreover, the soaking with PWA causes other hydrogen bond between four oxygen atoms of PWA and  $-\text{NH}_2$  or  $-\text{OH}$  groups of chitosan.

Fig. 2 shows the FTIR spectra of CS/PWA, CS/PWA-MMT, and CS/PWA-MMT/Sil membranes. The characteristic bands at 3420, 1650 and 1550  $\text{cm}^{-1}$  are attributed to hydroxyl group, amide I and amide II groups, respectively. The bands at 2894  $\text{cm}^{-1}$  attributed

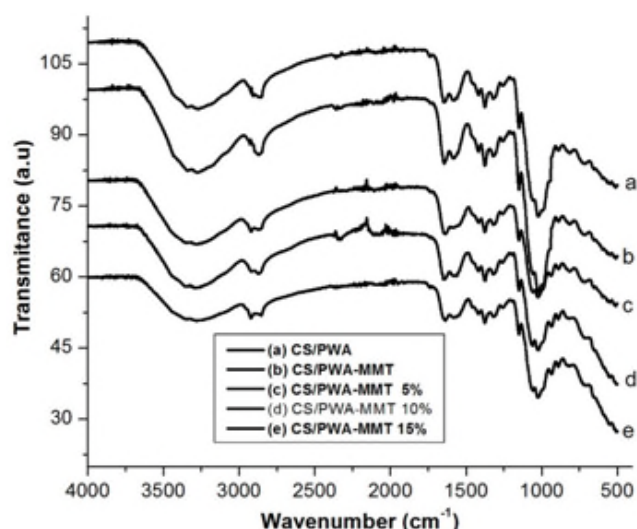


**Fig 2.** FT-IR spectra of CS/PWA, CS/PWA-MMT, and CS/PWA-MMT/Sil membranes

to C-H stretching vibration of  $-\text{CH}_2$  group and then shifted to 2922  $\text{cm}^{-1}$ . It is assigned to grafting silane in montmorillonite. The band at 1085  $\text{cm}^{-1}$  is attributed to Si-O-Si. The absorption band at 1070  $\text{cm}^{-1}$  and 1159  $\text{cm}^{-1}$  are due to the C-O stretching and asymmetric stretching of C-O-C [15,17]. The band at 1081  $\text{cm}^{-1}$  ( $\text{P-O}_a$ ), 967 ( $\text{W=O}_d$ ), 893  $\text{cm}^{-1}$  ( $\text{W-O}_b\text{-W}$ ), and 798  $\text{cm}^{-1}$  ( $\text{W-O}_c\text{-W}$ ) are attributed to PWA [23]. All the characteristic bands of PWA also appeared in the spectrum of complex-composite membranes. The intensity of the bands at 3420, 1650 and 1550  $\text{cm}^{-1}$  decrease in the complex-composite membranes spectrum because of the interaction between the  $-\text{OH}$ ,  $-\text{NH}_2$  groups on chitosan and  $-\text{OH}$  groups on modified-MMT as well as oxygen atoms on PWA.

### Water and Methanol Uptake

Water and methanol uptake of membranes have an important influence on their performance, such as proton conduction and methanol crossover. Fig. 3 showed the water and methanol uptake of CS/PWA-MMT and CS/PWA-MMT/Sil hybrid composite membranes. It can be observed that both water and methanol uptake decreased for CS/PWA-MMT/Sil 5% and CS/PWA-MMT/Sil 10% and slightly increased for CS/PWA-MMT 15% in hybrid composite membranes. This result should be attributes to two possible reasons: one is that the modified-montmorillonite less hydrophilic than the chitosan; the other is that the addition of the modified-montmorillonite rigidifies the chitosan chains, resulting in the decrease of their capability to adsorb the solvent molecules. In addition, the water uptake of all membranes is much higher than their methanol uptake, indicating that these membranes

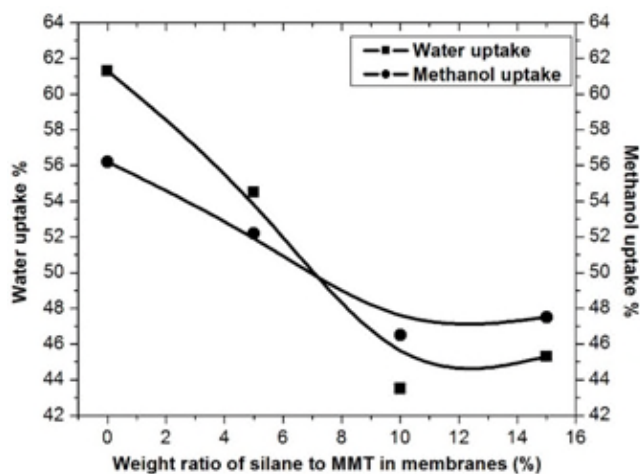


**Fig 3.** The water and methanol uptake curves of CS/PWA-MMT and CS/PWA-MMT/Sil membranes for various concentration of silane

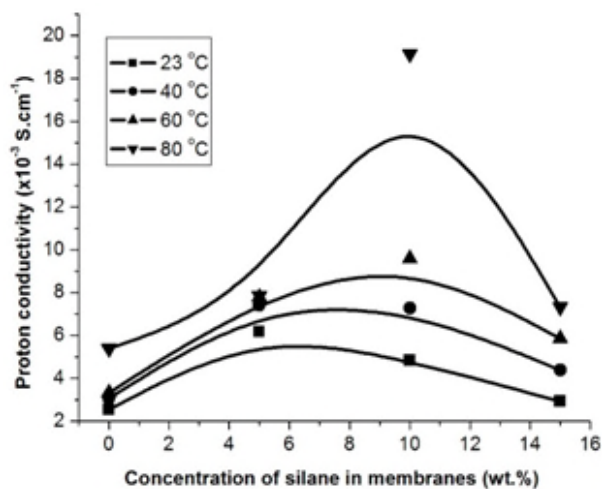


**Fig 4.** The proton conductivity vs. concentration of silane curves for various temperatures in membranes

**Table 1.** The proton conductivity of the CS/PWA, CS/PWA-MMT, and CS/PWA-MMT/Sil membranes at different temperatures.

Membrane	Proton conductivity ( $\times 10^{-3} \text{ S.cm}^{-1}$ )			
	23 °C	40 °C	60 °C	80 °C
CS/PWA	5.77	6.97	7.15	-
CS/PWA-MMT	2.55	3.07	3.33	5.39
CS/PWA-MMT/Sil 5%	6.17	7.42	7.78	7.85
CS/PWA-MMT/Sil 10%	4.84	7.28	9.59	19.15
CS/PWA-MMT/Sil 15%	2.92	4.38	5.86	7.32

have priority to adsorb water molecules. The decrease of both water and methanol uptake after grafting silane is caused by the adhesion and interface interaction between the montmorillonite and polymer is strengthened due to the surface modification of the montmorillonite [24]. Possible reason for increasing water and methanol uptake CS/PWA-MMT/Sil 15% is the adhesion and interface interaction between matrix polymer and filler become weak.

### Proton Conductivity

Proton conductivity of CS/PWA, CS/PWA-MMT, and CS/PWA-MMT/Sil membranes was determined by means of the complex impedance method. All impedances were carried out after hydration of the membranes. According to literature, proton conductivity will occur only after membrane is hydrate [16]. The proton conductivity data of the obtained CS/PWA, CS/PWA-MMT and CS/PWA-MMT/Sil membranes in various of temperature was listed in Table 1. It is noted that all membrane shows an increase of proton conductivity along with increase of temperature (see Fig. 5).

Fig. 4 shows the influence of silane concentration to proton conductivity CS/PWA-MMT and CS/PWA-MMT/Sil membranes at 23, 40, 60, and 80 °C. Generally,

the increase of silane concentration tends to increase the proton conductivity of CS/PWA-MMT/Sil membranes in all temperature operation. The highest proton conductivity is obtained to CS/PWA-MMT/Sil 10% at 80 °C. This result indicated that grafting silane onto montmorillonite surfaces with concentration 10% has the best compatibility between chitosan matrix and filler montmorillonite. This should be attributes to two possible reasons: one is that number of reactive groups which contribute as a "bridge" in proton transferring [25]. The CS/PWA-MMT membrane has lowest proton conductivity than CS/PWA-MMT/Sil due to it has less reactive groups which act as "bridge" in transferring proton. It is noted that interaction between epoxy groups (silane) and four type's oxygen (PWA) with amine groups (chitosan) through hydrogen bond contributed to transferring proton in membrane. Tohidian et al. [23] reported that interaction of hydrogen bond between amine groups in chitosan with four types of oxygen from phosphotungstic acid (PWA) in nanocomposite membranes based on PEC. These bridging and terminal oxygen are able to interact with protons and water molecules. In other side, the backbones from polysiloxane frameworks are able to interact with water molecules to facilitate transferring proton. Haidan et al. [26] reported that polysiloxane bonds in composite poly(ether-cetone-arylena) membrane

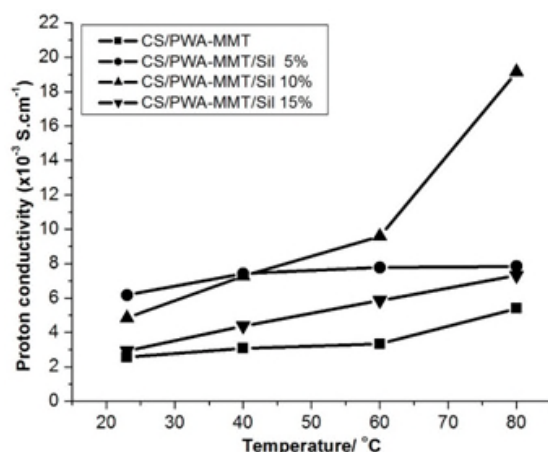


Fig 5. The proton conductivity vs. temperature curves in membranes

Table 2. Methanol permeability ( $P$ ) of CS/PWA and CS/PWA-MMT, CS/PWA-MMT/Sil membranes ( $A = 3.14 \text{ cm}^2$ )

Membrane	L (cm)	$P (x 10^{-8} \text{ cm}^2 \cdot \text{s}^{-1})$
CS/PWA	0.0015	9.55
CS/PWA-MMT	0.0016	5.09
CS/PWA-MMT/Sil 5%	0.0015	4.77
CS/PWA-MMT/Sil 10%	0.0017	4.33
CS/PWA-MMT/Sil 15%	0.0017	4.58

modified by silane are able to interact with water molecules to form water binding layer which facilitated proton hopping.

The second reason is water uptake, protons are largely transferred through the PEMs either as water-solvated species or by passing from one water molecule to another. Therefore, the ability of PEMs to imbibe large amount of water molecules enhances the proton conductivity in the most cases. Although, the highest water uptake also caused the decrease of proton conductivity especially in composite and hybrid system membrane is much more complex process as it involves both surface and chemical properties of the inorganic and organic phases [27]. In this case, the high migration of water into CS/PWA-MMT/Sil (0, 5 and 15%) membranes disturbed hydrogen bonding interaction between amine groups ( $-\text{NH}_2$ ) of chitosan with hydroxyl groups ( $-\text{OH}$ ) of montmorillonite and oxygen atoms of PWA. Tripathi and Shahi [28] said that the water content in membrane much required as proton transferring medium, but the overage of water content caused damaging interface properties of membrane. Peighambadoust et al. [27] also reported that the highest water content due to swell up of ion cluster, blowing up membrane, and damaged of bonding in membrane. It caused to decrease of proton line and proton migration is blocked, thus reduced the proton conductivity.

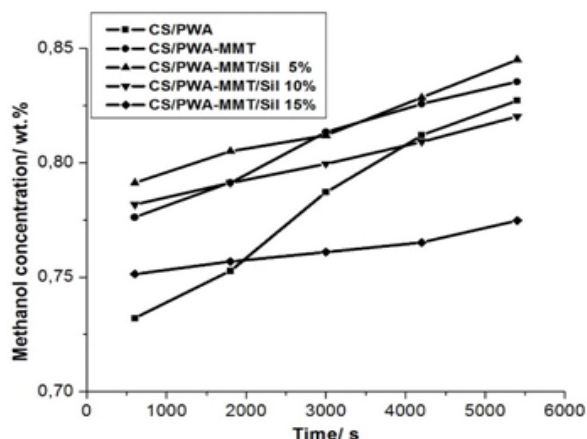


Fig 6. The methanol concentration vs. time curves for the CS/PWA membrane and CS/PWA-MMT membranes

In addition, this study observed the influence of operating temperature to proton conductivity. Fig. 5 shows the influence of temperature vs. proton conductivity membranes. As seen, the hybrid composite membranes generally show a significant increase in proton conductivity with increase in the temperature. The proton conductivity curves indicate similar trends with the water uptake behavior, which associated with the concurrent effects of PWA content and modified-MMT in the system. The increase of proton conductivity with increase temperature tends to electrochemical reaction occur faster, the enhanced of water production, and hydration process become much better, thus less resistance of membrane to ion is obtained. Therefore, the proton conductivity increases with increase in temperature [29]. The CS/PWA-MMT/Sil 10% membrane shows the highest proton conductivity  $19.15 \times 10^{-3} \text{ S.cm}^{-1}$  at  $80 \text{ }^\circ\text{C}$ . It is indicated that CS/PWA-MMT/Sil 10% membrane has the thermal and performance stability better than other membranes.

### Methanol Permeability

Fig. 6 shows the typical curve of methanol concentration vs. time for the CS/PWA, CS/PWA-MMT, and CS/PWA-MMT/Sil (5, 10 and 15%) membranes using 5 M  $\text{CH}_3\text{OH}$  aqueous solution. All values of methanol permeability tests for these complex-composite membranes were obtained from the slope of the straight line. It was found that the methanol permeability ( $P$ ) values of all complex-composite membranes were  $2.71\text{-}9.55 \times 10^{-8} \text{ cm}^2 \text{ s}^{-1}$ , respectively, as listed in Table 2.

As seen, CS/PWA membrane shows the highest methanol permeability. However, CS/PWA still has



lower methanol permeability than Nafion  $10 \times 10^{-6} \text{ cm}^2 \cdot \text{s}^{-1}$  [30]. The difference in the chemical and physical structure between Nafion and chitosan can account for this distinct difference in methanol permeation behavior. After incorporating montmorillonite into chitosan, the methanol permeability was further decreased. According to literature [15], this decrease may be attributed to the following two reasons: (1) the dispersion of inorganic particles increase the methanol permeation path length and tortuosity while the strong hydrophilic nature of montmorillonite present much more priority for water molecules traveling through the pores; (2) the incorporation of the rigid montmorillonite causes local rigidification of chitosan matrix and compresses the volumes between polymer chains, thus reducing the membrane swelling and methanol uptake.

The effect of montmorillonite modification with silane on the methanol barrier property can be clearly found. Compared with the CS/PWA-MMT membrane, the methanol permeability of CS/PWA-MMT/Sil membranes show the enhanced in methanol rejecting. It means that the compatibility between montmorillonite and polymer much better after grafting silane in montmorillonite surfaces. The transitional phase created the inorganic-polymer interface fills up the small voids and connects the two phases much closer. In addition, the reduction in montmorillonite pore size and total pore volume after modification is another favorable factor in increasing the water/methanol selectivity. This is result has similar trend with Wu et al. [15] that modified zeolite with APTES and MPTMS. Although the content of absorbed PWA, which also acts as the cross-linking agent in the membranes, was found to be decreased with increase in montmorillonite loading. As seen, the methanol permeability decreases while increase silane concentration and then slightly increased in CS/PWA-MMT/Sil 15%. This result indicates similar trends with methanol uptake. The lowest methanol permeability is obtained to CS/PWA-MMT/Sil 10% membrane.

## CONCLUSION

In conclusion, CS/PWA-MMT/Sil hybrid composite membranes were prepared through inversion phase method as function of various concentration of silane to modified montmorillonite. The resulting membranes were also visually transparent and homogenous. The increase of silane concentration from 5% to 15% caused the increase of proton conductivity, enhance methanol rejecting, but the decrease of water and methanol uptake.

The best composition of membrane was obtained in CS/PWA-MMT/Sil 10% with the highest proton conductivity and lower methanol permeability. However, the proton conductivity was still an order magnitude

lower than Nafion at  $3.84 \times 10^{-1} \text{ S} \cdot \text{cm}^{-1}$ . This result implies that this novel complex-composite membrane is a good candidate for DMFC in fuel cell application.

## ACKNOWLEDGEMENT

The first author is thankful to Directorate General of Higher Education (DIKTI) for their post-graduate scholarship. We thank to Dr. Bambang Prijamboedi and Multazam, M.Si., for their help in the proton conductivity measurements.

## REFERENCES

1. Hasani-Sadrabadi, M.M., Dasthimoghadam, E., Mokarram, N., Majedi, F.S., and Jacob, K.I., 2012, *Polymers*, 53 (13), 2643–2651.
2. Haghighi, A.M., Hasani-Sadrabadi, M.M., Dasthimoghadam, E., Bahlakeh, G., Shakeri, S.E., Majedi, F.S., Emami, S.H., and Moaddel, H., 2011, *Int. J. Hydrogen Energy*, 36 (5), 3688–3696.
3. Kreuer, K.D., 2001, *J. Membr. Sci.*, 185 (1), 29–39.
4. Wang, Y., Yang, D., Zheng, X., Jiang, Z., and Li, J., 2008, *J. Power Sources*, 183 (2), 454–463.
5. Su, Y.-H., Liu, Y.-L., Sun, Y.-M., Lai, J.-Y., Wang, D.-M., Gao, Y., Liu, B., and Guiver, M.D., 2007, *J. Membr. Sci.*, 296 (1-2), 21–28.
6. Di Vona, M.L., Ahmed, Z., Bellitto, S., Lenci, A., Traversa, E., and Licocchia, S., 2007, *J. Membr. Sci.*, 296 (1-2), 156–161.
7. Silva, V.S., Ruffmann, B., Silva, H., Silva, V.B., Mendes, A., Madeira, L.M., and Nunes, S., 2006, *J. Membr. Sci.*, 284 (1-2), 137–144.
8. Aricò, A.S., Baglio, V., Di Blasi, V., Creti, P., Antonucci, P.L., and Antonucci, V., 2003, *Solid State Ionics*, 161 (3-4), 251–265.
9. Rhee, C.H., Kim, H.K., Chang, H., and Lee, J.S., 2005, *Chem. Mater.*, 17 (7), 1691–1697.
10. Cui, Z., Liu, C., Lu, T., and Xing, W., 2007, *J. Power Source*, 167 (1), 94–99.
11. Chen, Z., Holmberg, B., Li, W., Wang, X., Deng, W., Munoz, R., and Yan, Y., 2006, *Chem. Mater.*, 18 (24), 5669–5675.
12. Sancho, T., Soler, J., and Pina, M.P., 2007, *J. Power Source*, 169 (1), 92–97.
13. Smitha, B., Sridhar, S., and Khan, A.A., 2005, *J. Membr. Sci.*, 259 (1-2), 10–26.
14. Smitha, B., Sridhar, S., and Khan, A.A., 2004, *Macromolecules*, 37 (6), 2233–2239.
15. Wu, H., Zheng, B., Zheng, X., Wang, J., Yuan, W., and Jiang, Z., 2007, *J. Power Sources*, 173 (2), 842–852.
16. Ramírez-Salgado, J. 2007, *Electrochim. Acta*, 52 (11), 3766–3778.

17. Ramadhan, L.O.A.N., Radiman, C.L., Suendo, V., Wahyuningrum, D., and Valiyaveettil, S., 2012, *Procedia Chem.*, 4, 114–122.
18. Wan, Y., Peppley, B., Creber, K.A.M., and Tam Bui, V., 2010, *J. Power Sources*, 195 (12), 3785–3793.
19. Salehi-Mobarakeh, H., Yadegari, A., Khakzad-Esfahlan, F., and Mahdavian, A., 2012, *J. Appl. Polym. Sci.*, 124 (2), 1501–1510.
20. Yang, C-C., Lee, Y-J., and Yang, J.N., 2009, *J. Power Sources*, 188 (1), 30–37.
21. He, H., Tao, Q., Zhu, J., Yuan, P., Shen, W., and Yang, S., 2013, *Appl. Clay Sci.*, 71, 15–20.
22. Su, L., Tao, Q., He, H., Zhu, J., Yuan, P., and Zhu, R., 2013, *J. Colloid Interface Sci.*, 391, 16–20.
23. Tohidian, M., and Ghaffarian, S.R., 2013, *J. Solid State Electrochem.*, 17 (8), 2123–2137.
24. Wang, Y., Jiang, Z., Li, H., and Yang, D., 2010, *Chem. Eng. Process. Process Intensif.*, 49 (3), 278–285.
25. Ma, J., and Sahai, Y., 2013, *Carbohydr. Polym.*, 92 (2), 955–975.
26. Lin, H., Zhao, C., Ma, W., Shao, K., Li, H., Zhang, Y., and Na, H., 2010, *J. Power Sources*, 195 (3), 762–768.
27. Peighambardoust, S.J., Rowshanzamir, S., and Amjadi, M., 2010, *Int. J. Hydrogen Energy*, 35 (17), 9349–9384.
28. Tripathi, B.P., and Shahi, V.K., 2011, *Prog. Polym. Sci.*, 36 (7), 945–979.
29. Belkhir, Z., Zeroual, M., Moussa, H., and Zitouni, B., 2011, *Revue des Energies Renouvelables*, 14 (1), 121–130.
30. Li, T., and Yang, Y., 2009, *J. Power Sources*, 187 (2), 332–340.